 doi:10.20944/preprints201804.0099.v1

Hot deformation behaviour of Cu/Al laminated composites under interface constraint effect

Shuaiyang Liu [a], Aiqin Wang [a, *], Tingting Liang [a], Jingpei Xie [a, b]

[a] School of Materials Science and Engineering, Henan University of Science and Technology, Luoyang 471023, China

[b] Collaborative Innovation Centers of Non-Ferrous Materials of Henan Province, Luoyang 471023, China

* Corresponding author. E-mail: aiqin_wang888@163.com

Abstract: In order to understand the hot deformation behavior of novel Cu/Al laminated composites, isothermal hot compression tests were conducted by Gleeble-1500D thermo-mechanical simulator. And the effect of bonding interface, deformation temperature and strain rate on the deformation behavior was analyzed. Results show that under the interface constraint effect, soft Al layer trends to flow synchronously with hard Cu layer. And further microstructure examinations indicate the cooperative deformation capability of Cu/Al composites increases with increasing stain rate and decreasing deformation temperature. Strain hardening exponent, calculated based on the true stress-true strain data, also proves the effect of deformation temperature and strain rate on the cooperative deformation behavior. Meanwhile, unique composites structure allows the Al matrix to exhibit the characteristic of dynamic recrystallization during the hot deformation process. Lastly, strain compensated Arrhenius-type constitutive equation was employed to describe the coupling effect of temperature, strain rate and strain on the flow stress.

Key words: Cu/Al laminated composites; deformation behavior; interface; microstructure; constitutive equation

1. Introduction

With the rapid development of modern industry, light-weight is an intense pursuit goal for more economical and green development at the basis of keeping original mechanical properties. Copper/aluminum (Cu/Al) laminated composites have been developed to meet these demands and several fabricate methods also have been presented in recent years [1-5]. Practices indicate that compared to monometallic copper or copper alloy, Cu/Al composites can reduce the weight of 40 ~ 50 %, save the cost of 30 ~ 50 % and keep almost consistent electrical and thermal conductivity [6]. Therefore, Cu/Al laminated composites have been utilized in a number of areas such as power, communication, architecture and aerospace [5, 7]. Until now, numerous studies about Cu/Al composites are mainly focused on the fabricate technologies [1-5], thermal treatment crafts [8-10] and bonding mechanisms [11, 12]. However, thermal mechanical machining such as hot rolling and tension also are necessary for Cu/Al composites in order to meet various industrial needs, to the authors' knowledge, related research is not available.

For the hot deformation behavior of metal materials, the essence is dynamic competition between work hardening and dynamic softening (including dynamic recrystallization and dynamic recovery), and the process is significantly affected by deformation temperature, strain rate, microstructure and so on [13]. Until now, Arrhenius-type constitutive equation is a kind of commonly used mathematical model to describe the relationship between the flow stress and deformation temperature, strain rate and deformation activation energy during the hot deformation process [14]. And the hot deformation behaviors of constituent metals of Cu/Al laminated composites have been investigated respectively through the Arrhenius-type constitutive equations [15-24].

Different from monometallic metal deformation behavior, the introduction of bonding interface usually will bring unique feature for composites. Such as, Patel *et al.* studied the compressive deformation behavior of AA2014 - 10 *wt*. % SiCp composites at the strain rate range of 0.01-10 s^{-1} and temperature range of 200 - 500 ℃. Microstructure features revealed that plastic incompatibility between the aluminum matrix and reinforcement lead to premature fracture of the composite [25]. Therefore, appropriate hot deformation parameters and processing map different from AA2014 aluminum alloy matrix have to been re-established for the SiCp reinforced aluminum

Preprints (www.preprints.org) | NOT PEER-REVIEWED | Posted: 9 April 2018 doi:10.20944/preprints201804.0099.v1

matrix composites [26, 27]. Nambu *et al*. investigated the relationship between the tensile ductility and interfacial bonding strength of multilayered steel composites and discovered that tensile ductility increased markedly with the increase of interfacial bonding strength [28]. Jiang *et al*. discovered that brittle high-Cr cast iron can deform like a ductile metal during the hot compression process of high-Cr cast iron/low carbon steel laminated composites, which benefits from the sound bonding interface between the two kinds of metals [29]. Here we expect that similar characters can also been found in the hot compression process of Cu/Al laminated composites.

In this paper, the isothermal compression deformation tests of Cu/Al laminated composites were conducted in the temperature range of 300 - 450 ℃ and strain rates range of 0.01 - 1 s^{-1}. Then, the collaborative deformation behaviors of Cu layer and Al layer were checked. The microstructure evolution of Al matrix during the isothermal compression process was investigated. Further, Cu/Al laminated composites with and without metallurgical bonding interfaces were compressed in same condition to explore the effect of interface on plastic flow behavior of Cu/Al laminated composites.

2. Material and experimental procedure

2.1. Material

Experimental Cu/Al laminated composites were produced by twin-roll casting technology. The thickness of Cu layer and Al layer are 1.5 mm and 8.5 mm, respectively, and the chemical components of them are list in Table 1. Meanwhile, in order to compare the deformation behavior of Cu/Al laminated composites and monometallic Al during the hot compression process, monometallic Al plate with a thickness of 10 mm was produced in the same twin-roll casting technology. The detailed casting procedures about Cu/Al composite plates have been reported in previous paper [30], after that the as-cast composites plate and monometallic Al plate were homogenized at 350℃ for 1 hour in an electrical resistance furnace. Then cylindrical specimens were machined from the homogenized sample with a diameter of 8 mm and height of 10 mm. And microstructure examination shows that ~ 3 μm thick interlayer has formed in the Cu/Al laminated composites due to the mutual diffusion between Cu and Al atoms, as shown in Fig. 1.

In order to investigate the effect of interface between Cu layer and Al layer on the compression deformation behavior of Cu/Al laminated composites, the cylindrical specimens were cut along the bonding interface using wire cut machine. Then, the cut surfaces of Cu layer and Al layer were polished and cleaned using a grade 600 abrasive paper and absolute ethanol, respectively. After that, the Al layer and Cu layer were simply put together again without any other further treatment. Next, the no-interface Cu/Al composite specimens will be compressed in same condition with the metallurgical bonding Cu/Al composites specimens.

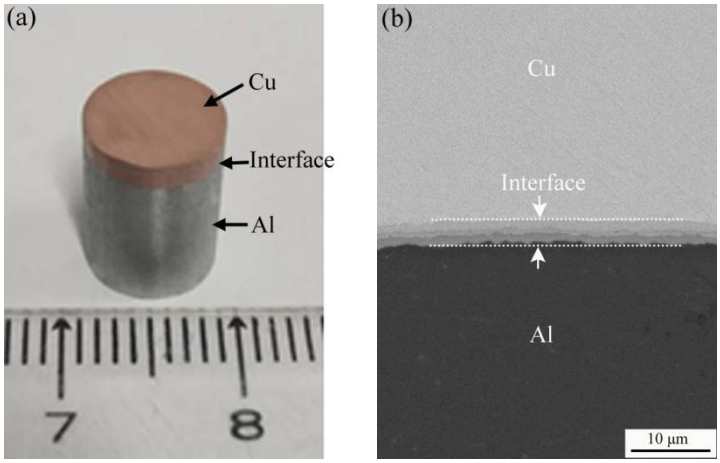

Fig.1 (a) Macro morphology of Cu/Al compression specimen and (b) microstructure of interface region

2.2. Isothermal compression

The isothermal compression experiments were conducted on a Gleeble-1500D thermo-mechanical simulator at constant temperatures of 300, 350, 400 and 450 ℃ and strain rate of 0.01, 0.1 and 1 s^{-1}, respectively. Prior to isothermal compression, graphite lubricant was used for reducing the friction between the specimen and the anvil.

Preprints (www.preprints.org) | NOT PEER-REVIEWED | Posted: 9 April 2018 doi:10.20944/preprints201804.0099.v1

Specimens were heated to the set temperature at a heating rate of 10 ℃/s and held for 60 s to eliminate the thermal gradients without increasing the thickness of Cu/Al interface. Subsequently, the specimens were compressed at a reduction rate of 50 %, and followed by water quenching to keep the deformed microstructure. The true stress-strain data were automatically collected by Gleeble-1500D thermo-mechanical simulator.

For microstructure observation, the compressed specimens were cut parallel to the compression axis through the center, and then the sectioned specimens were mechanically polished and the Al matrix was etched with 20% hydrofluoric acid (HF) solution. Microstructure observation was conducted on a Zeiss Axio Vert. A1 optical microscope.

Table 1 Chemical compositions of Cu plate and Al alloys

Alloys	Chemicals compositions (wt %)							
	Cu	Fe	Zn	S	P	Si	Mg	Al
Cu	99.96	0.0009	0.0008	0.0007	0.0009	0.0006	-	-
Al	0.04	0.16	0.04	-	-	0.17	0.04	99.5

3. Results and discussion

3.1 Compression deformation behavior

After hot compression, the typical cross sectional morphology of the deformed Cu/Al composite specimen is shown in Fig. 2a. As we can see, deformation mainly focuses on the soft Al layer and soft Al matrix was extruded during the hot compression process. Meanwhile, under the pressure stress in the vertical direction, the horizontal flow in different region of Al matrix is inhomogeneous. Obviously, the horizontal flow distance in bottom region of Al matrix is larger than that in top region (X_b>X_t), which may be ascribed to the constraint effect of Cu layer to Al layer through the bonding interface. For comparison, the no-interface Cu/Al composite specimen was compressed in the same deformation temperature and strain rate, as shown in Fig. 2b. Under this condition, the relative flow of Cu layer and Al layer on the interface region is obvious, even though the hard Cu layer has a friction drag effect on the soft Al layer, Al matrix flows faster in the horizontal direction (X_t >X_b). The distinction of the flowability of the Al matrix between these two kinds of hot compression specimens can well prove that interface plays an important role in the hot compression process of Cu/Al composites.

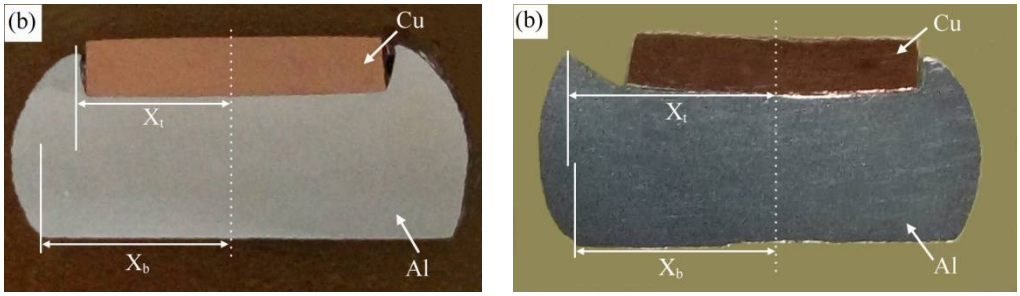

Fig. 2 The cross sectional morphology of hot deformed Cu/Al specimens (a) with and (b) without a bonding interface

Under the interface constraint, the plastic flow is inhomogeneous in different regions of Al matrix during the hot compression process. Further microstructure examination shows that the relative flow velocity of Al matrix almost reduces to zero on the interface region. As shown in Fig. 3a, the deformation degree of grains was not obvious. However, numerous of deformation textures, which are perpendicular to the compression axis, were found in the central region of Al matrix, which shows the relative flow in this region is serious, as shown in Fig. 3b. As we all known, in order to promote coordinated deformation of the bimetal laminated composites, the relative flow between these two kinds of materials should be as small as possible. Based on the difference of relative flow velocity and microstructure in different spots of Al matrix, we divided the aluminum matrix into three regions, as shown in Fig. 4. Further, naming the area Ⅰ, where the relative flow velocity is large, as easy-deformed region, and naming the area Ⅱ, where the relative flow velocity is small, as hard-deformed region.

For more uniform deformation during the hot compression process, we should try to reduce the scale of easy-deformed region. Comparing the deformation region of Cu/Al composite with and without a bonding

Preprints (www.preprints.org) | NOT PEER-REVIEWED | Posted: 9 April 2018 doi:10.20944/preprints201804.0099.v1

interface, the Cu/Al laminated composite with a bonding interface has a larger hard-deformed region in the interface region and littler easy-deformed region, which be ascribed to the constrain effect of hard Cu layer to softer Al layer through interface (Fig. 4). However, these two kinds of Cu/Al composites have similar hard-deformed region in the bottom of Al layer because of similar friction condition between specimen and anvil. Meanwhile, microstructure examination shows that deformation temperature and strain rate also have significant effect on the scale of deformed region of Cu/Al composites with a bonding interface, with the increase of strain rate or decrease of deformation temperature, the scale of hard-deformed region increases and the easy-deformed region decreases.

The hot compression deformation behavior of Cu/Al laminated composites is distinctly different from the tensile deformation behavior. During the tensile deformation process, the Cu layer, Al layer and interface layer suffer from equal strain, and brittle interface layer will fracture firstly due to weak ductility. Subsequently, the Cu layer and Al layer will fracture separately [31]. However, during the hot compression process, deformation happens in the softer and thicker Al layer firstly because of isostress behavior. Then, Al layer will put tension stress on the Cu layer and Cu layer will also enforce compressive stress on Al layer so that they can deformation simultaneously. Obviously, sound bonding interface between Cu layer and Al layer promotes the possible of coordinate deformation of dissimilar metals. Meanwhile, in the horizontal direction, little strain gradient between Cu layer and Al layer on the interface region will not produces large shear stress to destroy the interlayer.

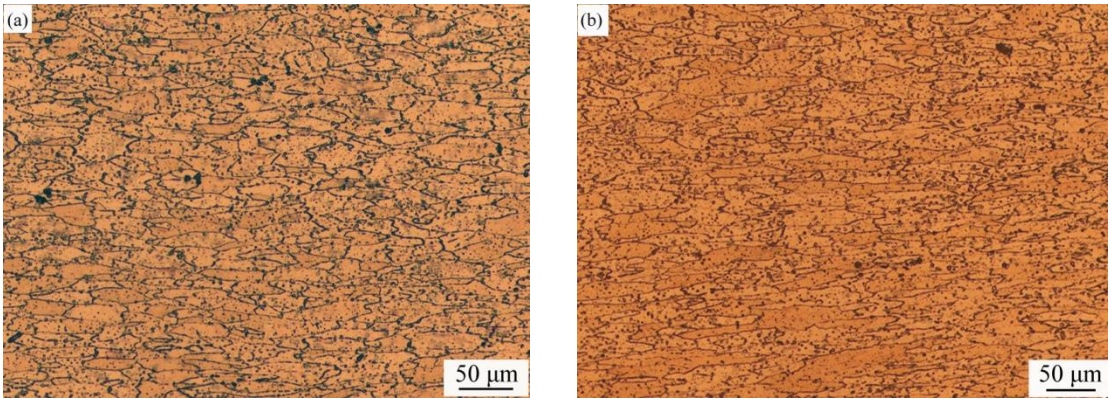

Fig. 3 Microstructures of different regions after hot compression at 450 ℃/0.01s^{-1}: (a) interface region and (b) central region of Al matrix

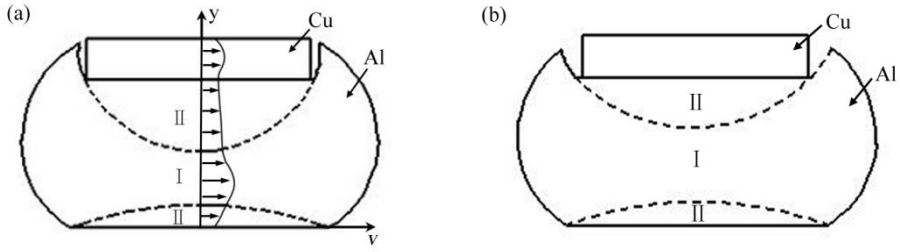

Fig. 4 Schematic diagrams of different deformation regions in Cu/Al composites (a) with and (b) without a bonding interface (Ⅰ: easy-deformed region, Ⅱ: hard-deformed region)

3.2 True stress- true strain curves

The true stress-true strain curves of Cu/Al laminated composites and monometallic Al at different deformation temperatures and strain rates are shown in Fig. 5. Similar with the property of other Al alloy, deformation temperature and strain rate have remarkable effect on the flow stress of both Cu/Al laminated composites and monometallic Al. And flow stress increases with increasing strain rate or decreasing deformation temperature [15, 32, 33]. What makes the Cu/Al laminated composite apart from monometallic Al is the variation tendency of flow stress. During the beginning stage of deformation, the flow stress of Cu/Al composites increases dramatically and reaches peak stress at an extremely small strain (~ 0.01). However, the flow stress of

Preprints (www.preprints.org) | NOT PEER-REVIEWED | Posted: 9 April 2018 doi:10.20944/preprints201804.0099.v1

monometallic Al increases slowly and reaches a peak stress at a large strain (~ 0.06). Furthermore, at low deformation temperature, like 300℃ and 350℃, the flow stress of Cu/Al composite and monometallic Al will continue to increases after reaching peak stress, indicating work hardening always plays a dominant role. But as for the Cu/Al laminated composites, with the further increase of strain, faster increase of flow stress produces a large amount of deformation heating so that dynamic softening starts to plays a dominant role at certain strain and then flow stress exhibits a dropping tendency, showing the feature of dynamic recrystallization. Obviously, the deformation heating originated from work hardening in monometallic Al is not enough to counteract the work hardening so that flow stress increases monotonously with increasing strain. The difference can be ascribed to the interface puts strong resistance to dislocation slip during the hot compression process of Cu/Al laminated composites, which does not exist in the hot compression process of monometallic Al. At high hot deformation temperature, like 400℃ and 450℃, the thermally activated process strongly controls the hot deformation process, atomic movement and dislocation slip become easy. At this time, softening mechanism starts to play a dominant role once the flow stress reaches peak during the hot compression process of Cu/Al laminated composites. Unfortunately, the constraint effect of interface on the flow of softening Al layer is weakened at such a high deformation temperature. Because the deformation mainly focuses on the softer Al layer, combined with weak effect of interface, the flow stresses of Cu/Al laminated composites are similar with the monometallic Al during the hot compression process at high temperature.

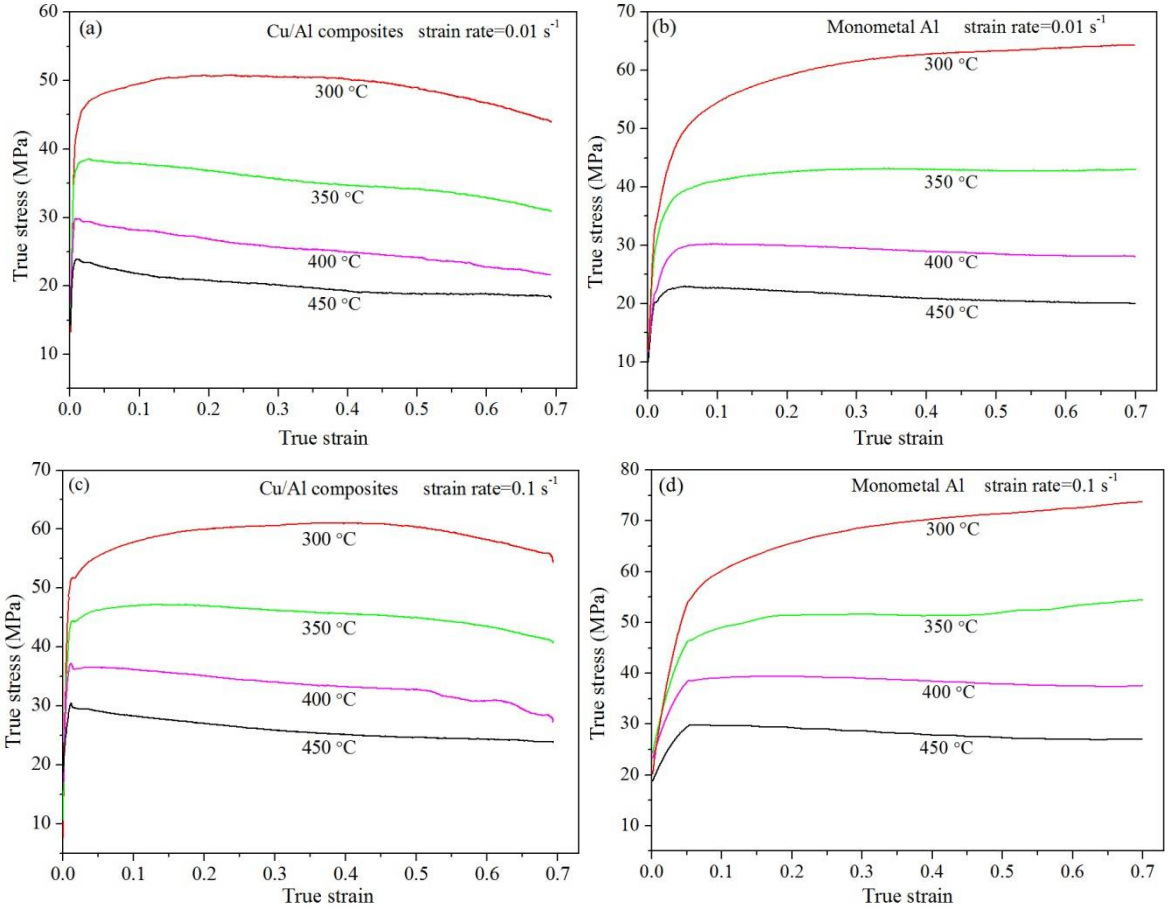

Preprints (www.preprints.org) | NOT PEER-REVIEWED | Posted: 9 April 2018 doi:10.20944/preprints201804.0099.v1

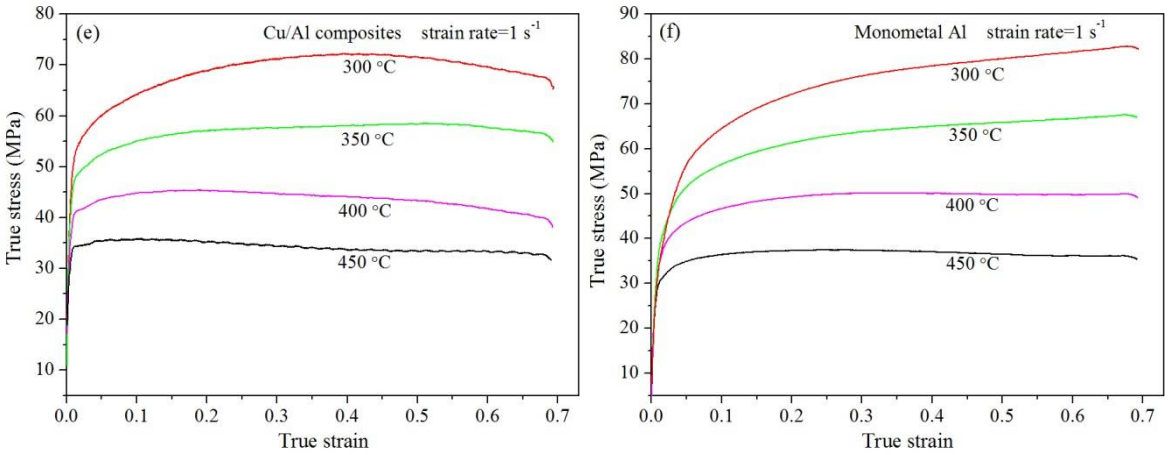

Fig. 5 True stress–strain curves of Cu/Al composites and monometal Al under different strain rates of (a) 0.01 s^{-1}, (b) 0.1 s^{-1} and (c) 1 s^{-1}

Further, the work hardening and dynamic softening mechanisms of Al matrix in Cu/Al laminated composites were confirmed by the optical micrographs. At low deformation temperature and high strain rate (Fig.6a)，work hardening play a dominant role until a high strain value so that deformed grains were elongated greatly, and deformation textures make the grain boundary almost invisible. With the increase of deformation temperature (Fig.6b)，dynamic softening mechanism can counteract the work hardening mechanism at early stage of hot compression, new undistorted grains have enough time to nucleate and can be found around the grain boundaries, which meets the feature of dynamic recrystallization. At high deformation temperature and low strain rate (Fig.6c), there is more time and energy for the dislocations slipping and climbing. More recrystallization grains have formed and grown up.

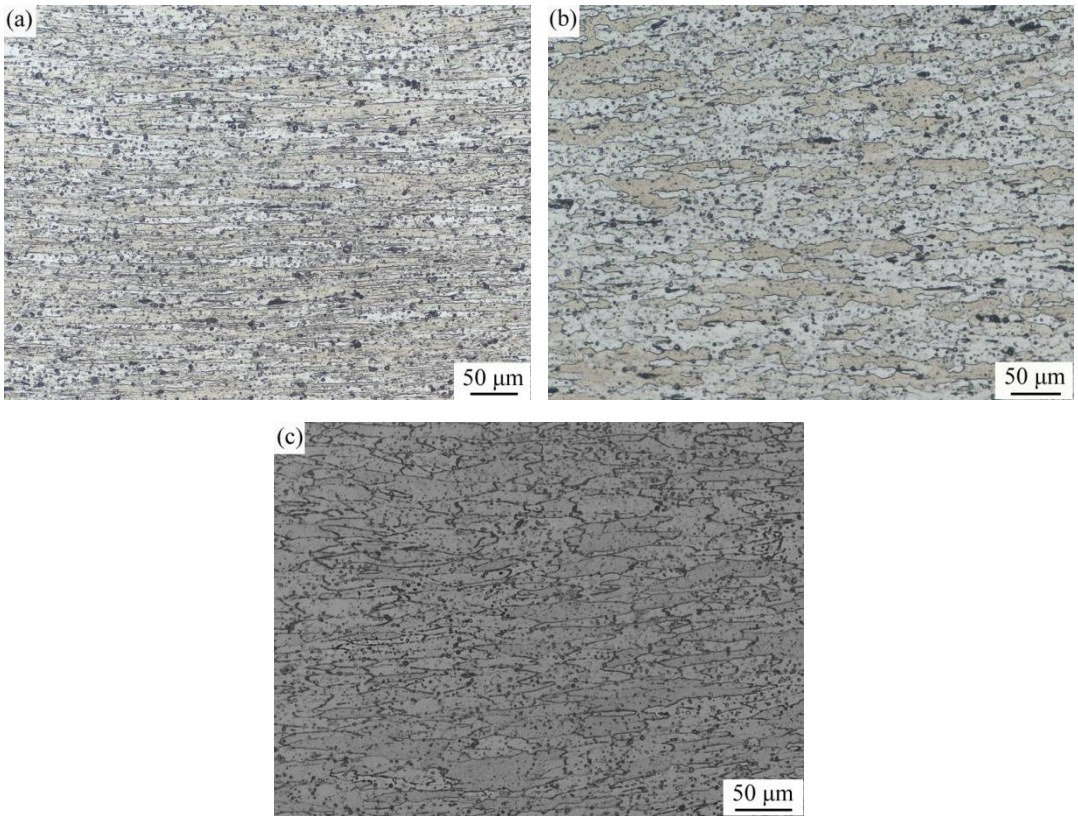

Fig.6 Microstructure of Al matrix in Cu/Al laminated composites after compressed under different conditions: (a) 300˚C/0.1s^{-1}, (b) 450˚C/0.1s^{-1} and (c) 450˚C/0.01s^{-1}

3.3 Strain hardening behavior

It is well known that the uniform plastic deformation ability of a material is related to the strain hardening capacity, which can be enhanced by increasing storage of dislocations or weakened by dynamic softening

Preprints (www.preprints.org) | NOT PEER-REVIEWED | Posted: 9 April 2018 doi:10.20944/preprints201804.0099.v1

mechanism, like dynamic recovery and dynamic recrystallization [34]. Meanwhile, the increase or reduction of dislocations are related to the deformation temperature, strain rate and deformation degree [35]. That means the ductility of a material can be improved by applying optimal combination of deformation temperature, strain rate and deformation degree. Based on characteristics, the mathematical model of strain hardening exponent n, considering the effect of deformation temperature and strain rate, was proposed to evaluate the homogeneous deformation ability of a material during the deformation process [36]. As expressed in Eq. (1).

$$n = \frac{\partial \operatorname{Ln} \sigma}{\partial \operatorname{Ln} \varepsilon}\Big|_{T,\dot{\varepsilon}} \tag{1}$$

As we can see, strain hardening exponent n will be a positive value when the stress increases with the increase of strain under constant deformation temperature and strain rate, which shows that the work hardening plays a dominant role at this time. And strain hardening exponent n will be a negative value when the stress decreases with the increase of strain under constant deformation temperature and strain rate, which shows that the dynamic softening plays a dominant role at this time. Specifically, the effect of strain on strain hardening exponent n during the hot compression process of Cu/Al laminated composites is shown in Fig. 7. As seen from Fig. 7, the strain hardening exponent n gradually decreases even become negative with the increase of strain, which shows that the work hardening mechanism plays a dominant role at the beginning stage of isothermal compression of Cu/Al laminated composites, however with the increase of strain, a amount of deformation heating was produced so that the dynamic softening mechanism can gradually balance the work hardening effect and play a leading role. Especially at deformation temperature of 400 ℃ and 450 ℃, the strain hardening exponent n are negative over all of the deformation processes, which shows the dynamic softening mechanism plays a dominant role from the beginning of isothermal compression process (Fig. 7b). Furthermore, it is noted that both decreasing deformation temperature and increasing strain rate can enhance the strain hardening exponent n, which results in the positive strain hardening exponent extending to a higher strain degree. Therefore, hot compression tests of Cu/Al laminated should be conducted at low deformation and high strain rate for more uniform deformation. Now, the calculation results can well agree with the microstructure observation.

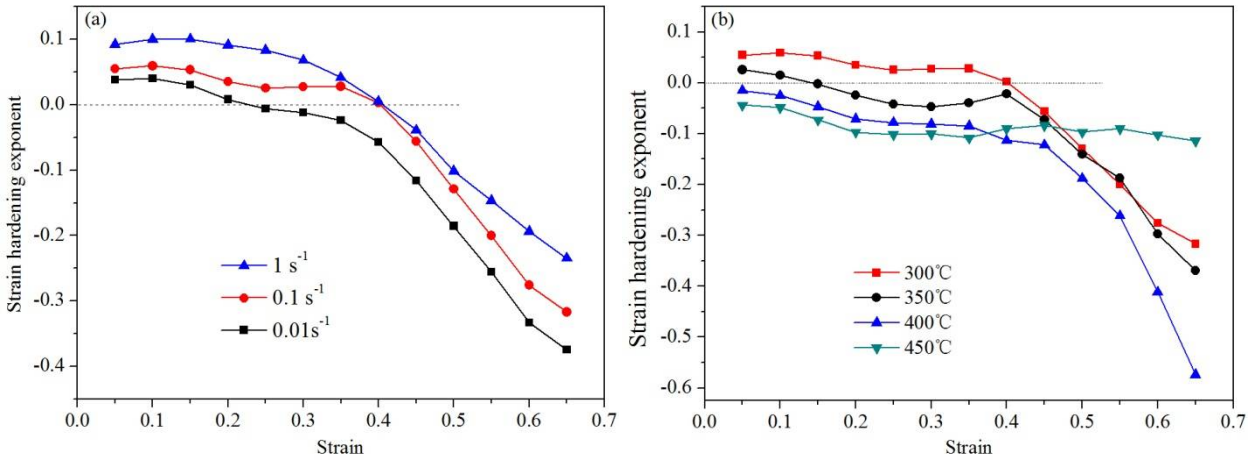

Fig. 7 The effect of strain on the strain hardening exponent n during hot compression process of Cu/Al laminated composites at (a) deformation temperature of 300 ℃ and (b) strain rate of 0.1s^{-1}

3.4 Modeling the hot deformation behavior

3.4.1 Constitutive model

The Arrhenius-type equation, considering the relation between strain rates, deformation temperatures, stress and deformation activation energy, generally is used to describe the metal flow behavior, as Eq. (2).

$$\dot{\varepsilon} = A[\sinh(\alpha\sigma)]^n \exp\left(-\frac{Q}{RT}\right) \tag{2}$$

Where A, α and n are material constants, $\dot{\varepsilon}$ is the strain rate (s^{-1}), σ is the flow stress (MPa), Q is the deformation activation energy (KJ/mol), R is the gas constant (8.314 KJ/ (mol · K)), and T is the deformation temperature (K).

Preprints (www.preprints.org) | NOT PEER-REVIEWED | Posted: 9 April 2018 doi:10.20944/preprints201804.0099.v1

During the hot deformation process, Eq. (2) can be used in all stress level. However, for the lower stress level, Eq. (3) is more suitable. And for higher stress level, Eq. (4) is fit to describe the relation between strain rate and flow stress.

$$\dot{\varepsilon} = A_1 \sigma^{n_1} \exp\left(-\frac{Q}{RT}\right) \tag{3}$$

$$\dot{\varepsilon} = A_2 \exp(\beta\sigma) \exp\left(-\frac{Q}{RT}\right) \tag{4}$$

Where, A_1, n_1, A_2 and β are material constants. Meanwhile, Eqs. (3) and (4) can be translated into Eqs. (5) and (6) by taking the natural logarithm on both side.

$$\ln \dot{\varepsilon} = n_1 \ln \sigma + \ln A_1 - \frac{Q}{RT} \tag{5}$$

$$\ln \dot{\varepsilon} = \beta\sigma + \ln A_2 - \frac{Q}{RT} \tag{6}$$

Then, the flow stresses and strain rates under the true strain of 0.4 are submitted to Eqs. (5) and (6). It is obvious that $\ln \dot{\varepsilon}$-$\ln \sigma$ and $\ln \dot{\varepsilon}$-σ meet some linear relation at constant deformation temperatures because A_1, n_1, A_2 and β all are constants. Then, the fitted lines under different temperatures are illustrated in Fig. 8 and the values of n_1 and β were calculated respectively from the average slop. Further, the constant α can be attained as $\alpha = \beta / n_1$, the value of it is 0.0254 MPa^{-1}.

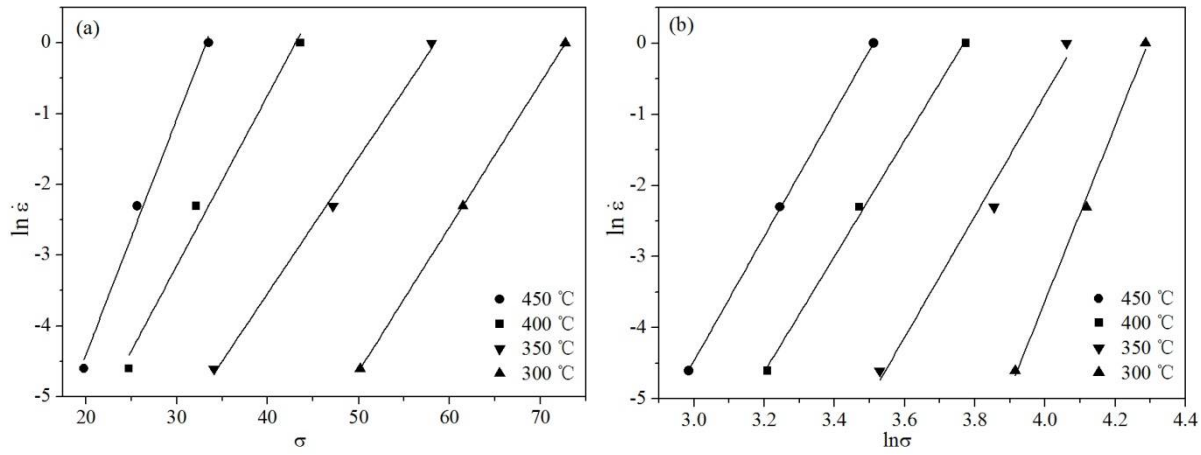

Fig.8 (a) $\ln \dot{\varepsilon}$-σ and (b) $\ln \dot{\varepsilon}$-$\ln \sigma$ plots at different deformation temperatures

Taking the natural logarithm of both sides of Eq. (2), Eq. (7) can be attained. $\mathrm{Ln}\,\dot{\varepsilon}$-$\ln[\sinh(\alpha\sigma)]$ plot also meets a linear relation under constant deformation temperature, as shown in Fig. 9a. Substituting the values of strain rate and flow stress, the average slop n over the range of deformation temperature was found to be 6.90.

$$\ln \dot{\varepsilon} = n \ln[\sinh(\alpha\sigma)] + \ln A - \frac{Q}{RT} \tag{7}$$

The hot deformation activation Q, which indicates the deformation difficulty degree of test material and is the critical energy value of starting the dislocation movement [37, 38], can be calculated by taking partial differential of Eq. (7), as shown in Eq. (8).

$$Q = R\left[\frac{\partial \ln \dot{\varepsilon}}{\partial \ln[\sinh(\alpha\sigma)]}\right]_T \cdot \left[\frac{\partial \ln[\sinh(\alpha\sigma)]}{\partial(1/T)}\right]_{\dot{\varepsilon}} = RnL \tag{8}$$

The parameter L represents the average slop of $\ln[\sinh(\alpha\sigma)]$-$1/T$ plot under test temperatures. By substituting the values of flow stress and deformation temperature under constant strain rate, the value of L be calculated and it is 3249.44 (Fig. 9b). Therefore, the activation energy (Q) can be obtained to be 186.43 KJ/mol. It was higher than that for self-diffusion of commercial pure aluminum (126.45 KJ/mol), and even higher than that of AA2014 - 10 *wt*. % SiCp composite (168 KJ/mol) [15, 25]. Such obvious increase of Q values shows the effect of composites structure on the deformation activation energy is significant. According to Eq. (2), at constant strain rate and

Preprints (www.preprints.org) | NOT PEER-REVIEWED | Posted: 9 April 2018 doi:10.20944/preprints201804.0099.v1

deformation temperature, flow stress increases with increasing Q values, which means the deformation of Cu/Al laminated composites needs larger force, that correspond with the fact that interface has constraint effect on flow of Al matrix.

Meanwhile, the Zener-Hollomon equation can also be utilized to represent the coupling effect of strain rate and deformation temperature, as Eq. (9).

$$Z = \dot{\varepsilon}\exp\left(\frac{Q}{RT}\right) = A[\sinh(\alpha\sigma)]^n \tag{9}$$

Taking the natural logarithm of both sides of Eq. (9):

$$\ln Z = \ln A + n\ln[\sinh(\alpha\sigma)] \tag{10}$$

Then, substituting the solutions of α and Q, the values of ln Z and ln [sinh($\alpha\sigma$)] under different strain rates and deformation temperatures can be calculated and the relationship of them can be further plotted, as shown in Fig.10. The good linear relationship demonstrates the possibility that building a mathematical model about the strain rate, deformation temperature and stress, so that the plastic deformation behavior can be expressed clearly.

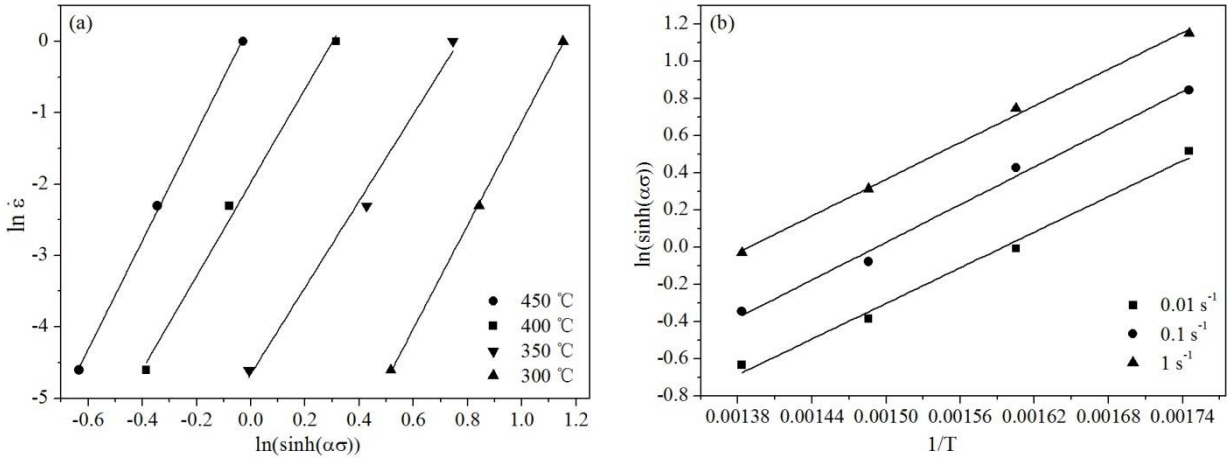

Fig.9 (a) ln $\dot{\varepsilon}$-ln[sinh($\alpha\sigma$)] plots at different temperatures, (b) ln[sinh($\alpha\sigma$)]-1/T plots at different strain rate

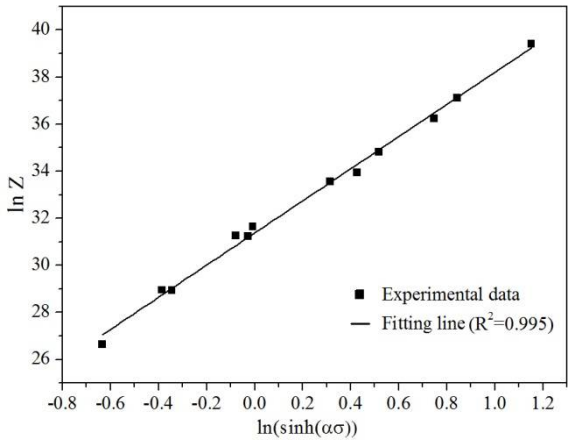

Fig.10 Relationship between ln Z and ln [sinh($\alpha\sigma$)]

3.4.2 Modified constitutive model

As shown in Fig.5, the flow stresses alter dramatically with the increase of deformation strain, especially in lower deformation temperature such as 300 and 350 ℃. However, the foundation of the constitutive equation is the equilibrium between the work hardening and the dynamic softening, and the flow stress varies little with the increase of strain. That mean the effect of strain on stress cannot be ignored anyway in this paper. Therefore, the constitutive equation built according to the parameters of strain 0.4 is not representative over the all strain situations. The compensation of strain should be taken into account when computing the material constants (A, α, n and Q) so that the flow stress can be predicted more accurately [32, 39, 40].

Preprints (www.preprints.org) | NOT PEER-REVIEWED | Posted: 9 April 2018 doi:10.20944/preprints201804.0099.v1

Using the same calculation method, the material constants are calculated again at the strain range of 0.05 ~ 0.65 at the interval of 0.05. Further, the relationship between these material constants and true strain can be polynomial fitted, as shown in Fig.11. The order of polynomial was experimented from 2 to 9 and result shows that 5 order polynomial fitting the experimental data very well, the polynomial are shown in Eq. (11) and the polynomial coefficients are list in Table 2.

$$\begin{cases} \alpha(\varepsilon) = \mathrm{B}_0 + \mathrm{B}_1\varepsilon + \mathrm{B}_2\varepsilon^2 + \mathrm{B}_3\varepsilon^3 + \mathrm{B}_4\varepsilon^4 + \mathrm{B}_5\varepsilon^5 \\ n(\varepsilon) = \mathrm{C}_0 + \mathrm{C}_1\varepsilon + \mathrm{C}_2\varepsilon^2 + \mathrm{C}_3\varepsilon^3 + \mathrm{C}_4\varepsilon^4 + \mathrm{C}_5\varepsilon^5 \\ Q(\varepsilon) = \mathrm{D}_0 + \mathrm{D}_1\varepsilon + \mathrm{D}_2\varepsilon^2 + \mathrm{D}_3\varepsilon^3 + \mathrm{D}_4\varepsilon^4 + \mathrm{D}_5\varepsilon^5 \\ ln\ A(\varepsilon) = \mathrm{E}_0 + \mathrm{E}_1\varepsilon + \mathrm{E}_2\varepsilon^2 + \mathrm{E}_3\varepsilon^3 + \mathrm{E}_4\varepsilon^4 + \mathrm{E}_5\varepsilon^5 \end{cases} \tag{11}$$

Table 2 Coefficients of polynomial for α, n, Q and ln A.

α coefficient	n coefficient	Q coefficient	ln A coefficient
B_0 = 2.5409	C_0 = 12.3182	D_0 = 209.4480	E_0 = 34.9790
B_1 = -2.2942	C_1 = -47.5148	D_1 = -191.4209	E_1 = -28.2479
B_2 = 14.0243	C_2 = 192.5064	D_2 = 370.7157	E_2 = 35.9870
B_3 = -31.8606	C_3 = -420.2749	D_3 = 903.3894	E_3 = 232.5851
B_4 = 31.7676	C_4 = 460.1838	D_4 = -3544.5115	E_4 = -714.7760
B_5 = -10.2397	C_5 = -199.5526	D_5 = 2675.6823	E_5 = 514.9587

At this time, strain modified constitutive equations can accurately describe the deformation behavior of Cu/Al laminated composites at different strain rates, deformation temperatures and strains, as shown in Eq. (12).

$$\dot{\varepsilon} = A(\varepsilon)[\sinh(\alpha(\varepsilon)\sigma)]^{n(\varepsilon)}\exp\left(-\frac{Q(\varepsilon)}{RT}\right) \tag{12}$$

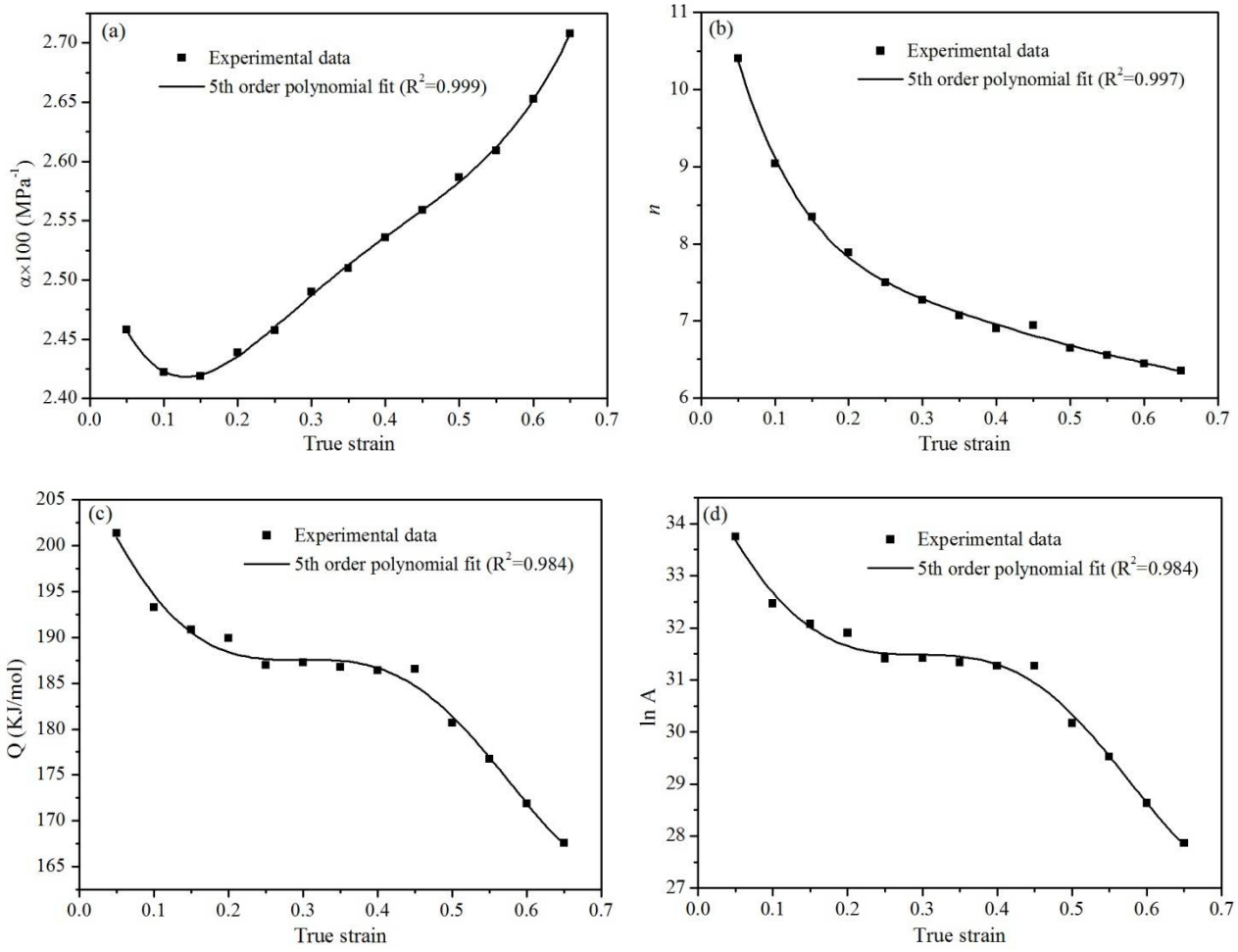

Preprints (www.preprints.org) | NOT PEER-REVIEWED | Posted: 9 April 2018 doi:10.20944/preprints201804.0099.v1

Fig.11 Relationship between (a) α, (b) n, (c) Q and (d) ln A with true strain by polynomial fit of Cu/Al composite plate

3.4.3 Verification of the modified constitutive model

Based on the strain modified constitutive models, the flow stress values can be calculated precisely and compared with the experimental flow stress, as shown in Fig. 12. It can be observed that the predicated and the experimental stress values have a satisfactory match at almost all the deformation temperatures and strain rates. In order to further verify the accuracy of the modified constitutive model, the correlation coefficient (R) and average absolute relative error ($AARE$) also are computed. They are expressed as follows:

$$R = \frac{\sum_{i=1}^{N}(E_i - \bar{E})(P_i - \bar{P})}{\sqrt{\sum_{i=1}^{N}(E_i - \bar{E})^2 \sum_{i=1}^{N}(P_i - \bar{P})^2}} \tag{13}$$

$$AARE(\%) = \frac{1}{N}\sum_{i=1}^{N}\left|\frac{E_i - P_i}{E_i}\right| \times 100 \tag{14}$$

Where N is the total number of the calculated stress values over the entire experimental temperatures and strain rates, E_i is the measured flow stress values, P_i is the calculated flow stress values, $\bar{E}$ and $\bar{P}$ are the average values of E_i and P_i, respectively.

Fig. 13 shows the strength of linear relationship between the experimental and predicated flow stress values. Then, the correlation coefficient (R) can be obtained as high as 0.9976. Meanwhile, average absolute relative error ($AARE$), an unbiased statistical parameter, also was calculated to be only 1.84%. The high correlation coefficient and low average absolute relative error collectively indicate the high accuracy of the modified constitutive model. Therefore, it is reasonable to believe that the developed constitutive model in this paper can accurately describe the flow behavior of the Cu/Al laminated composites at elevated temperature and strain rate.

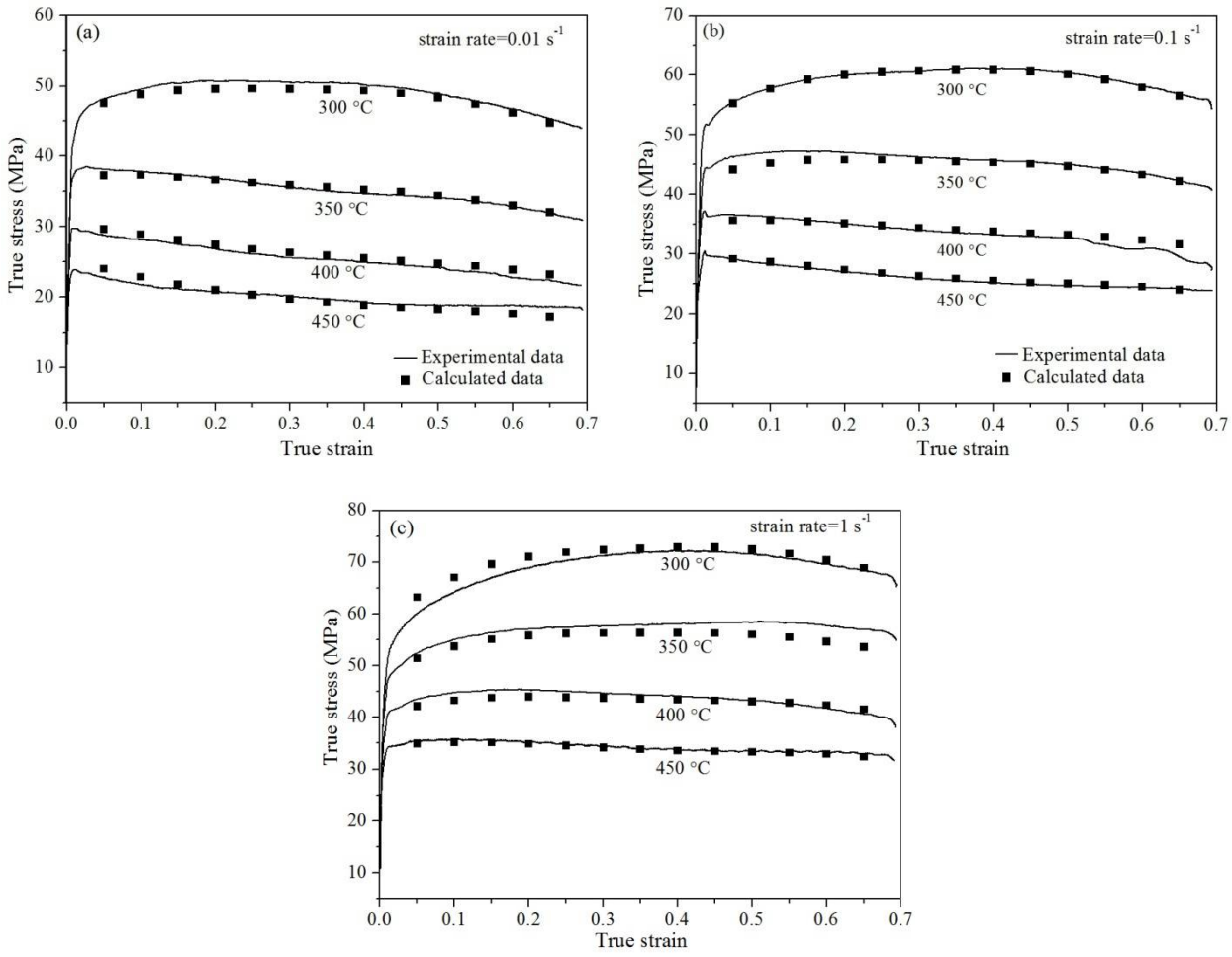

Fig.12 Comparisons between the measured and predicted flow stress of Cu/Al composite plate at strain rates of (a) 0.01 s^{-1}; (b) 0.1 s^{-1};

Preprints (www.preprints.org) | NOT PEER-REVIEWED | Posted: 9 April 2018 doi:10.20944/preprints201804.0099.v1

(c) 1 s^{-1}

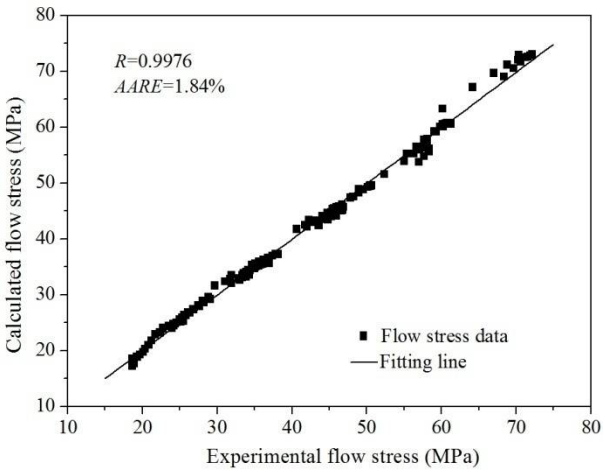

Fig. 13 The correlation between the experimental and calculated flow stress values from the modified constitutive model

4. Conclusions

In this paper, the isothermal hot compression tests of a novel Cu/Al laminated composites were conducted in the temperature range of 300 ~ 450 ℃ and strain rate range of 0.01 ~ 1 s^{-1}. The flowing conclusions can be obtained from the study.

(1) Under the interface constraint effect, soft Al layer and hard Cu layer will coordinate each other during the hot compression process of Cu/Al composites materials. And the cooperative deformation capability increases with increasing stain rate and decreasing deformation temperature.

(2) In order to keep coordinated deformation during the hot compression process, hard Cu layer will put strong tension stress on the soft Al layer and significantly increase the dislocation slip resistance, so that a large amount of deformation heating makes the dynamic softening mechanism of Al matrix conform to the characteristics of dynamic recrystallization.

(3) Strain hardening exponent *n* was calculated based on the true stress-true strain data. And calculation results show that Cu/Al composites can achieve more coordinated deformation at low deformation temperature and high strain rate, which agrees with the microstructure observation.

(4) The deformation activation energy of the studied Cu/Al composites materials is greater than that of pure Al, which can be ascribed to the influence of interface.

(5) The strain compensated constitutive equation can match the experimental values very well. High correlation coefficient and low average absolute relative error show that the modified constitutive equation can accurately predict the deformation behavior of Cu/Al composites.

Acknowledgements

This study was financially supported by the National Natural Science Foundation of China (Grant No. U1604251).

References

[1] Pintore M, Starykov O, Mittler T, Volk W, Tonn B. Experimental Investigations on the Influence of the Thermal Conditions During Composite Casting on the Microstructure of Cu–Al Bilayer Compounds. International Journal of Metalcasting. 2017:1-10.

[2] Li X, Zu G, Wang P. Interface strengthening of laminated composite produced by asymmetrical roll bonding. Materials Science & Engineering A. 2013;562:96-100.

[3] Liu T, Wang Q, Sui Y, Wang Q, Ding W. An investigation into interface formation and mechanical properties of aluminum–copper bimetal by squeeze casting. Materials & Design. 2016;89:1137-46.

[4] Hoseini-Athar MM, Tolaminejad B. Interface morphology and mechanical properties of Al-Cu-Al laminated composites

fabricated by explosive welding and subsequent rolling process. Metals & Materials International. 2016;22:670-80.

[5] Gao HT, Liu XH, Qi JL, Ai ZR, Liu LZ. Microstructure and mechanical properties of Cu/Al/Cu clad strip processed by the powder-in-tube method. Journal of Materials Processing Technology. 2018;251:1-11.

[6] Kim IK, Sun IH. Effect of heat treatment on the bending behavior of tri-layered Cu/Al/Cu composite plates. Materials & Design. 2013;47:590-8.

[7] Sasaki TT, Morris RA, Thompson GB, Syarif Y, Fox D. Formation of ultra-fine copper grains in copper-clad aluminum wire. Scripta Materialia. 2010;63:488-91.

[8] Chen CY, Hwang WS. Effect of annealing on the interfacial structure of aluminum-copper joints. Materials Transactions. 2007;48:1938-47.

[9] Honarpisheh M, Asemabadi M, Sedighi M. Investigation of annealing treatment on the interfacial properties of explosive-welded Al/Cu/Al multilayer. Materials & Design. 2012;37:122-7.

[10] Li X, Zu G, Ding M, Mu Y, Wang P. Interfacial microstructure and mechanical properties of Cu/Al clad sheet fabricated by asymmetrical roll bonding and annealing. Materials Science & Engineering A. 2011;529:485-91.

[11] Guo Y, Liu G, Jin H, Shi Z, Qiao G. Investigation on the Interfacial Structure and Phase Formation Mechanism of the Diffusion-Bonded Cu/Al Laminates. Rare Metal Materials & Engineering. 2011;40:215-20.

[12] Li H, Chen W, Dong L, Shi Y, Liu J, Fu YQ. Interfacial Bonding Mechanism and Annealing Effect on Cu-Al Joint Produced by Solid-Liquid Compound Casting. Journal of Materials Processing Technology. 2018;252.

[13] Lin YC, Dong WY, Zhou M, Wen DX, Chen DD. A unified constitutive model based on dislocation density for an Al-Zn-Mg-Cu alloy at time-variant hot deformation conditions. Materials Science & Engineering A. 2018.

[14] Prasad YVRK. Processing maps: A status report. Journal of Materials Engineering & Performance. 2003;12:638-45.

[15] Ashtiani HRR, Parsa MH, Bisadi H. Constitutive equations for elevated temperature flow behavior of commercial purity aluminum. Materials Science & Engineering A. 2012;545:61-7.

[16] Sun PL, Cerreta EK, Iii GTG, Bingert JF. The effect of grain size, strain rate, and temperature on the mechanical behavior of commercial purity aluminum. Metallurgical & Materials Transactions A. 2006;37:2983-94.

[17] Airod A, Vandekinderen H, Barros J, Colás R, Houbaert Y. Constitutive equations for the room temperature deformation of commercial purity aluminum. Journal of Materials Processing Technology. 2003;134:398-404.

[18] Malas JC, Venugopal S, Seshacharyulu T. Effect of microstructural complexity on the hot deformation behavior of aluminum alloy 2024. Materials Science & Engineering A. 2004;368:41-7.

[19] Deng Y, Yin Z, Huang J. Hot deformation behavior and microstructural evolution of homogenized 7050 aluminum alloy during compression at elevated temperature. Materials Science & Engineering A. 2011;528:1780-6.

[20] He J, Zhang D, Zhang W, Qiu C, Zhang W. Constitutive Equation and Hot Compression Deformation Behavior of Homogenized Al-7.5Zn-1.5Mg-0.2Cu-0.2Zr Alloy. Materials. 2017;10:1193.

[21] Li M, Jiang QW. The effect of strain rates on tensile deformation of ultrafine-grained copper. International Journal of Modern Physics B. 2017:1744014.

[22] Zhang H, Zhang HG, Peng DS. Hot deformation behavior of KFC copper alloy during compression at elevated temperatures. Transactions of Nonferrous Metals Society of China. 2006;16:562-6.

[23] Bahmanpour H, Kauffmann A, Khoshkhoo MS, Youssef KM, Mula S, Freudenberger J, et al. Effect of stacking fault energy on deformation behavior of cryo-rolled copper and copper alloys. Materials Science & Engineering A. 2011;529:230-6.

[24] Zhu AY, Chen JL, Zhou LI, Luo LY, Lei Q, Zhang L, et al. Hot deformation behavior of novel imitation-gold copper alloy. Transactions of Nonferrous Metals Society of China. 2013;23:1349-55.

[25] Patel A, Das S, Prasad BK. Compressive deformation behaviour of Al alloy (2014)–10 wt.% SiC p composite: Effects of strain rates and temperatures. Materials Science & Engineering A. 2011;530:225-32.

[26] Hao SM, Xie JP, Wang AQ, Wang WY, Ji-Wen LI, Sun HL. Hot deformation behaviors of 35%SiC p /2024Al metal matrix composites. Transactions of Nonferrous Metals Society of China. 2014;24:2468-74.

[27] Zhang P, Li F, Wan Q. Constitutive Equation and Processing Map for Hot Deformation of SiC Particles Reinforced Metal Matrix Composites. Journal of Materials Engineering & Performance. 2010;19:1290-7.

[28] Nambu S, Michiuchi M, Inoue J, Koseki T. Effect of interfacial bonding strength on tensile ductility of multilayered steel

composites. Composites Science & Technology. 2009;69:1936-41.

[29] Zheng-yi, JIANG, Xing-jian, Sheng-li, Hong-mei, ZHANG, et al. Interface Analysis and Hot Deformation Behaviour of a Novel Laminated Composite with High-Cr Cast Iron and Low Carbon Steel Prepared by Hot Compression Bonding. Journal of Iron and Steel Research, International. 2015;22:438-45.

[30] Huang HG, Dong YK, Yan M, Feng-Shan DU. Evolution of bonding interface in solid–liquid cast-rolling bonding of Cu/Al clad strip. Transactions of Nonferrous Metals Society of China. 2017;27:1019-25.

[31] Li XB, Yang Y, Xu YS, Zu GY. Deformation behavior and crack propagation on interface of Al/Cu laminated composites in uniaxial tensile test. Rare Metals. 2018:1-8.

[32] Haghdadi N, Zarei-Hanzaki A, Abedi HR. The flow behavior modeling of cast A356 aluminum alloy at elevated temperatures considering the effect of strain. Materials Science & Engineering A. 2012;535:252-7.

[33] Wu H, Wen SP, Huang H, Wu XL, Gao KY, Wang W, et al. Hot deformation behavior and constitutive equation of a new type Al–Zn–Mg–Er–Zr alloy during isothermal compression. Materials Science & Engineering A. 2016;651:415-24.

[34] Tan HF, Zhang B, Luo XM, Sun XD, Zhang GP. Strain rate dependent tensile plasticity of ultrafine-grained Cu/Ni laminated composites. Materials Science & Engineering A. 2014;609:318-22.

[35] Li J, Wang B, Huang H, Fang S, Chen P, Shen J. Unified modelling of the flow behaviour and softening mechanism of a TC6 titanium alloy during hot deformation. Journal of Alloys & Compounds. 2018.

[36] Hollomon JH, Member J. Tensile Deformation. Metals Technology. 1945;12:268-90.

[37] Mokdad F, Chen DL, Liu ZY, Ni DR, Xiao BL, Ma ZY. Hot deformation and activation energy of a CNT-reinforced aluminum matrix nanocomposite. Materials Science & Engineering A. 2017;695:322-31.

[38] Xiang S, Liu DY, Zhu RH, Jin-Feng LI, Chen YL, Zhang XH. Hot deformation behavior and microstructure evolution of 1460 Al-Li alloy. Transactions of Nonferrous Metals Society of China. 2015;25:3855-64.

[39] Gao XJ, Jiang ZY, Wei DB, Li HJ, Jiao SH, Xu J, et al. Constitutive analysis for hot deformation behaviour of novel bimetal consisting of pearlitic steel and low carbon steel. Materials Science & Engineering A. 2014;595:1-9.

[40] Lin YC, Wen DX, Deng J, Liu G, Chen J. Constitutive models for high-temperature flow behaviors of a Ni-based superalloy. Materials & Design. 2014;59:115-23.